Developments in the FBK Production of Ultra-Fast Silicon Detectors

M. Ferrero, O.H. Ali, R. Arcidiacono, M. Boscardin, N. Cartiglia, F.Cenna, R. Cirio, M. Costa, G.F. Dalla Betta, F.Ficorella, S. Giordanengo, M. Mandurrino, V. Monaco, M.M. Obertino, L. Pancheri, G. Paternoster, R. Sacchi, F. Siviero, V. Sola, A. Staiano, A. Vignati

Abstract–In this contribution we present new developments in the production of Ultra Fast Silicon Detectors (UFSD) at Fondazione Bruno Kessler (FBK) in Trento, Italy. FBK after having in 2016 a successfully first production of UFSD sensors 300-micrometer thick, has produced in 2017 its first 50-micrometer thick UFSD sensors. These sensors use high resistivity Silicon on Silicon substrate and have different doping profile configurations of the gain layer based on Boron, Gallium, Carbonated Boron and Carbonated Gallium to obtain a controlled multiplication mechanism. The motivation of variety of gain layers it is to identify the most radiation hard technology to be employed in the production of UFSD for applications in high-radiation environments.

I. INTRODUCTION

Ultra-Fast Silicon Detector (UFSD) is an innovative silicon sensor optimized for timing measurements [1], [2] based on the Low-Gain Avalanche Diode technology (LGAD). LGAD merges the best characteristics of traditional silicon sensor with the main features of Avalanche Photodiode (APD). LGAD is a silicon detector with output signal about a factor 10 larger than that of standard silicon detector and with noise comparable with that of traditional silicon sensor. The LGAD technology was first proposed by the Center of Microelectronica National (CNM, Barcelona) [3-5]. UFSDs have recently obtained in beam test a time resolution $\sigma_t \sim 30$ ps [6]; a review of the development of UFSD for timing measurement in charge particle tracking can be found in [4].

The charge multiplication in silicon sensors needs an electric field of the order of $E \sim 300$ kV/cm, under this condition the electrons (and to less extent the holes) acquire enough kinetic energy that is able to generate additional e/h pairs. A field value of 300 kV/cm is not reachable applying an external voltage bias without causing an electrical breakdown,

but it is obtained by implanting an appropriate charge density that locally generates very high electric field. The additional $p+$ doping layer ($N_A \sim 10^{16}/cm^3$) is implanted under the $n++$ cathode, the $p+/n++$ junction in the LGAD design, Fig. 1, allows to achieve the electric field necessary to get the avalanche charge multiplication.

II. DEVELOPMENT IN UFSD PRODUCTION AT FONDAZIONE BRUNO KESSLER (FBK)

The first production of UFSD at FBK was completed in 2016 on a 300 μm substrate, this production included several type of structure AC and DC-coupled devices [7], [8]. The key aspect of this first production is the good control of the low gain mechanisms and the good correspondence between measurements and simulations of the gain as a function of the gain layer doping. The good comparison between data and simulation showed the successful of this first production.

In 2017 FBK applied the technological know-how gained in the 300 μm thick production to thinner substrates. FBK manufactured UFSD on 50 μm thick Si-on-Si high resistivity substrates (6 inch wafer), establishing a reliable design for UFSD on thin substrates.
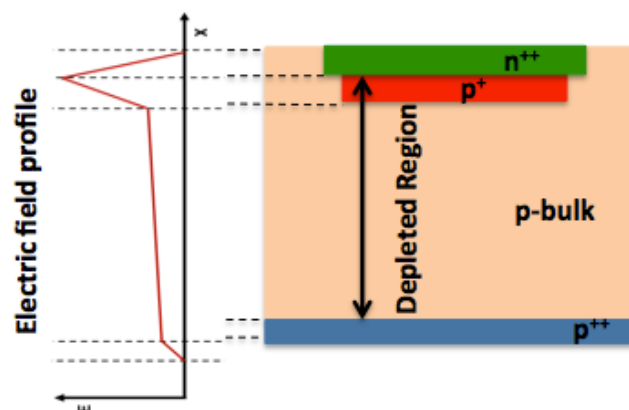

Fig. 1. Schematic of Low-Gain Avalanche Diode.

Recent radiation damage studies on UFSD from different manufactures show that the doping of the gain layer becomes progressively deactivated by irradiation. The exact nature of this effect is not known, it has been shown that the boron atoms are still present in the gain layer, but they switch from substitutional to interstitial, therefore do not contribute to the gain mechanism. A proposal in the latest RD50 meeting [9] has been to replace the Boron doping of the gain layer with Gallium and/or to add high level of Carbon ($\sim 10^{18} -$

$10^{19}/cm^3$) in the gain layer volume to reduce the disappearance of gain. Gallium has a lower probability to become interstitial than Boron, while Carbon has a higher probability to become interstitial protecting the Boron (or Gallium) dopant. Gallium implant and activation required a new complete simulation, since implantation energy and diffusion velocity are different from there of Boron.

In the latest 50 µm production of UFSD at FBK, we have simulated and manufactured devices with 4 different gain layer configuration: (i) Boron, (ii) Boron with Carbon, (iii) Gallium, and (iv) Gallium with Carbon. The Boron implant has been divided in 4 doping concentration of the gain layer (arbitrary scale, step of 2%) and also in two different diffusion temperature, the Gallium implant instead has been divided in 3 doping concentration of the gain layer (arbitrary scale, step of 4%): the Carbon implant has been divided in two level of concentration (high and low level). Table I, summarize the characteristics of UFSD 50 µm thick production at FBK.
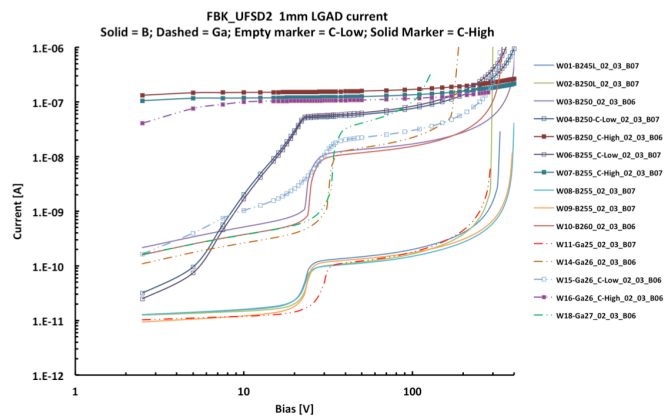

Fig. 2. Reverse current for different wafers as a function of the applied voltage.
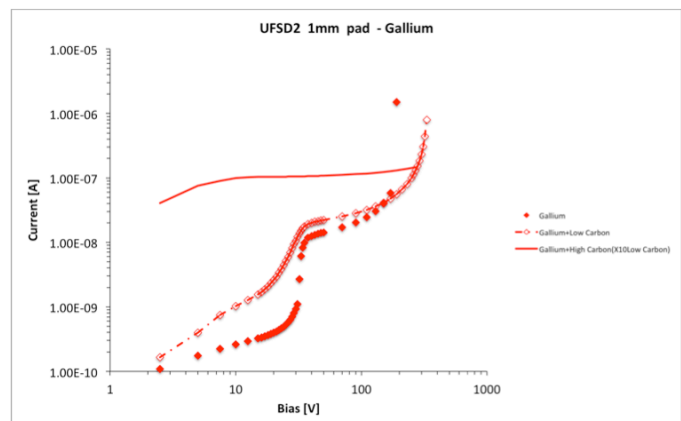

Fig. 3. Reverse current on wafers with p+ Gallium implant and high Carbon implant (solid line), low Carbon implant (empty marker) and without Carbon (solid marker). Sensors with p+ implant of Boron have very similar measurements.

TABLE I. UFSD 50µM PRODUCTION

Wafer #	Dopant	Gain Dose	Carbon	Diffusion
1	Boron	0.98		Low
2	Boron	1.00		Low
3	Boron	1.00		High
4	Boron	1.00	Low	High
5	Boron	1.00	High	High
6	Boron	1.02	Low	High
7	Boron	1.02	High	High
8	Boron	1.02		High
9	Boron	1.02		High
10	Boron	1.04		High
11	Gallium	1.00		Low
12	Gallium	1.00		Low
13	Gallium	1.04		Low
14	Gallium	1.04		Low
15	Gallium	1.04	Low	Low
16	Gallium	1.04	High	Low
18	Gallium	1.08		Low
19	Gallium	1.08		Low

III. SENSORS, MEASUREMENTS AND RESULTS

The sensors used to characterize the FBK production of UFSDs are single pad sensors with an active area 1 mm x 1 mm.

A. Reverse Current

Fig. 2, Shows the reverse current of the UFSDs at room temperature, performed on sensors with all the four different configurations of the gain layer. These measurements were performed on the wafers before being cut. The reverse current shows three different trends as a function of reverse voltage. Below 20 V the measured current is a surface current, between 20 V and 30 V the current show a skip due to the depletion of the gain layer and above 30 V the leakage current has an exponential trend due to the relationship between gain and bias voltage. The two families of current in Fig. 2, (high and low current), are due to two different batches of wafers.

The addition of Carbon atoms to the gain layer does not modify the electrical characteristic of UFSDs, however it increases the leakage current of the sensors Fig. 3. This effect is more significant for high level of Carbon concentration. For low Carbon concentration ($\sim 10^{18}/cm^3$) the shape of the leakage current trend is the same as that of sensors without Carbon, instead for high Carbon concentration ($\sim 10^{19}/cm^3$) the leakage current is higher, with different shape Fig. 3.

B. Capacitance Versus Voltage

A planar silicon sensor with a reverse bias, can be considered a parallel plate capacitor. The distance between the capacitor's plates is the width of the depletion region and the area of the plate is the active area of the sensor. The capacitance (C) of a planar silicon sensor is a function of the reverse voltage (V) and of acceptors active doping concentration (N_A). This relationship is shown in (1).

$$C \propto \sqrt{N_A/V} \qquad (1)$$

The measurement of capacitance on UFSD, Fig. 4, shows a capacitance drop, this drop matches with the full depletion on the gain layer an with the starting depletion of the p-bulk. There is a relationship between the position on the voltage

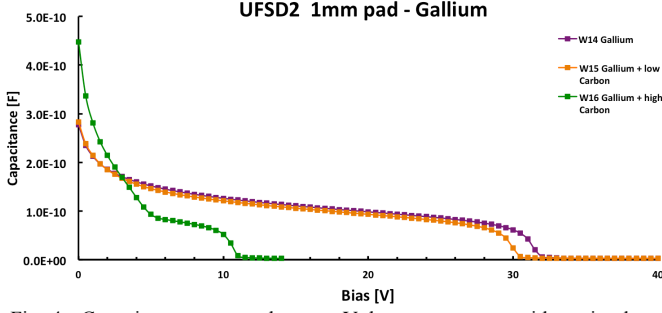axes of this drop and the active doping concentration of the gain layer.

Fig. 4. Capacitance measured versus Voltage on sensors with p+ implant of Gallium (violet), of Gallium-low Carbon (orange) and of Gallium-high Carbon (green). Sensors with p+ Boron implant have a very similar measurement.

Fig. 4, show that the presence of Carbon atoms shifts to lower voltage the position of the capacitance drop. This means that there is an inactivation of the active doping concentration of the $p+$ implant, therefore a loss of gain is expected. The loss of gain due to the implant of the Carbon increases with carbon concentration, Fig. 4.

C. Gain Measurement

The method used to measure the gain (G) of UFSD, defined in (2), Fig. 5, is the Transient Current Technique (TCT). TCT induces a signal into the sensor using a picosecond laser. The laser is focused with a spot diameter of 50 μm and a wavelength of 1060 nm.

$$G = Signal\ Area\ UFSD / Signal\ Area\ Diode \qquad (2)$$

The output signal of UFSD is amplified by a factor 100 using a Cividec Broadband amplifier. The signal was acquired by a Lecroy Oscilloscope (740Zi) with a sampling of 40 GSample/s and a bandwidth of 4 GHz.
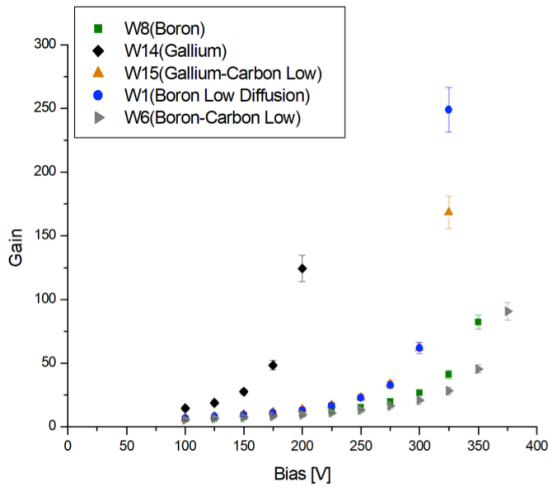

Fig. 5. Gain as a function of the voltage measured on 5 sensors with different configuration of the gain layer, Boron (green), Gallium (black), Gallium-low Carbon (orange), Boron low diffusion (blue) and Boron-low Carbon (grey).

The gain has an exponential dependency on the electric field and therefore on the bias voltage [1]. Gain measurements show two important results:

- Boron low diffusion has a higher gain than Boron high diffusion. The explanation of this result is the different doping profile between high and low diffusion implants as expected by Montecarlo simulation.
- Carbon presence reduces the gain, both for Boron and Gallium p+ implant, in agreement with the measurements on the capacitance. Gain reduction is more pronounced on sensors with Gallium implant than Boron.

IV. TIME RESOLUTION

The time resolution σ_t (3) can be expressed as the sum of several terms: (i) Jitter σ_{Jitter}, (ii) Landau Time Walk $\sigma_{Land.TW}$, (iii) Landau noise $\sigma_{Land.noise}$ due to shape variation, (iv) signal distortion $\sigma_{Dist.}$.

$$\sigma_t^2 = \sigma_{Jitter}^2 + \sigma_{Land.TW}^2 + \sigma_{Land.noise}^2 + \sigma_{Dist.}^2 \qquad (3)$$

We will assume three simplifications:

- The effect of time walk can be compensated using Constant Fraction Discriminator (CFD) analysis.
- In silicon sensors the shape of the signal can be calculated using Ramo's theorem [1], [2]. The signal induced by a charge carrier is proportional to the drift velocity of the charge and to the weighting field into the sensor. The signal distortion can be neglected if the drift velocities of electrons and holes are saturated and if the weighting field is very uniform.

Therefore with these three simplifications the predominant terms of the time resolution are Jitter and Landau noise.

A. Jitter

The jitter term represents the time uncertainty caused by the presence of noise and the signal slope. The jitter component (4) is directly proportional to the noise N and inversely proportional to the slope dV/dt of the signal.

$$\sigma_{Jitter} = \frac{N}{dV/dt} \qquad (4)$$

Fig. 6, shows the measurements of the jitter noise as a function of the gain. This measurement was performed using TCT and using the same amplification and acquisition chain used on the gain measurements. For this measurement, the laser attenuation was set to replicate the charge most probable value induced by a Minimum Ionizing Particle (MIP). The Jitter component decreases as the increases gain, and it reaches values between 50 ps to 20 ps for gain 15 to 35.

The measurement of the jitter was performed on sensors with three different configuration of the gain layer (i) Boron low diffusion, (ii) Boron and (iii) Gallium-Carbon low Concentration. Doping type of the gain layer does not affect the performances of the sensors.
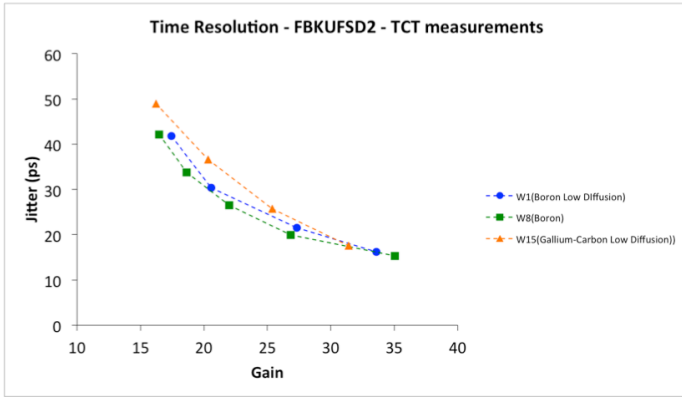
Fig. 6. Jitter as a function of the gain measured on sensors with three different gain layer configurations, Boron (green), Boron low diffusion (blue) and Gallium-low Carbon (orange).

B. Landau Noise

Ionizing particles crossing a sensor create a different charge distribution on an event-to-event basis, this variation produces an irregular current signal. The landau noise contribution to the time resolution depends to the sensor thickness and for a sensor of 50 µm thick is about 30 ps.

The time resolution on three sensors (Boron, Boron low diffusion and Gallium-low Carbon) was measured in a beam test. The beam was 180 GeV/c Pions and the trigger used for the data acquisition was the signal of a calibrated UFSD (50 µm thickness with a time resolution of 35 ps. The acquisition chain used during the beam test was the same of the gain and jitter measurements.
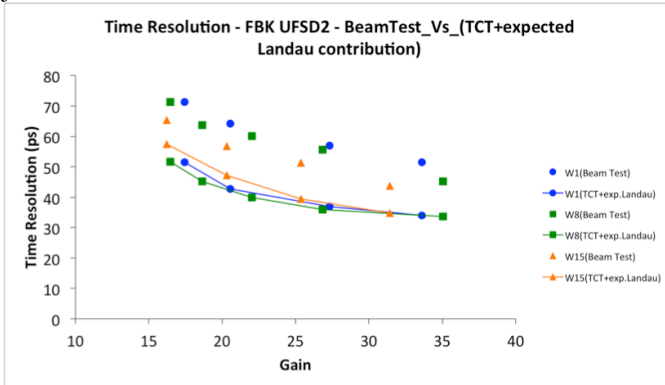

Fig. 7. Time resolution expected by jitter an landau noise (dots-line), time resolution measured in a beam test.

Time resolutions extrapolated by the data analysis using the CFD technique is between 70 ps and 45 ps in a gain range between 15 and 35. This time resolution is 20 ps larger than the expected value by jitter and landau noise. Data analysis is ongoing.

V. SENSORS DEAD AREA

Pixelated UFSD needs to have good gain termination at the edge of each pixel. An important parameter in strip and multi-pad sensors is the dead area between active area. The dead area characterization on this FKB production has been performed on strip sensors.

The strips under test have a width of 150 µm and a pitch of 220 µm. The measure technique used for the characterization was the Edge-TCT. It consist in injection a focused pulsed laser on the edge of the sensor. The laser has a wavelength of 1060 nm and during the measure the spot diameter was 12 µm.
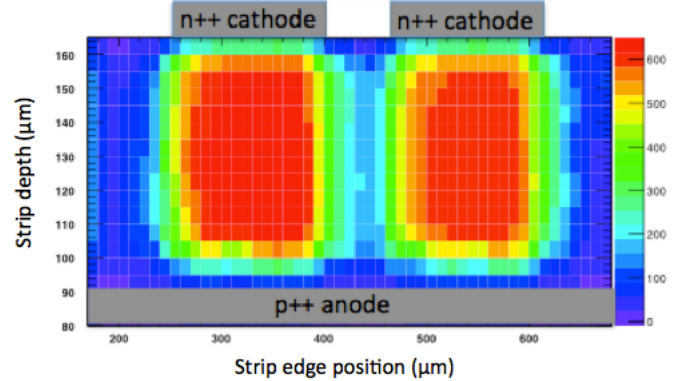

Fig. 8. Edge scan of the strip sensor acquired with the TCT setup, on the x axes the strip edge position, on the y axes the strip depth, color scale represents the signal amplitude.
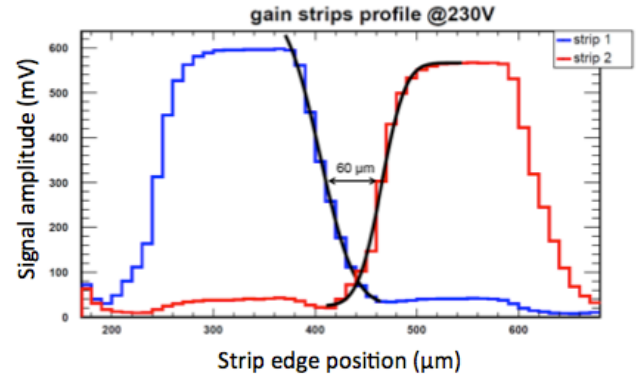

Fig. 9. Signal amplitude as a function of the edge position through two strips.

Fig. 8, is the 2D plot of the edge scan of the strip sensor: there is a clear disjunction between the two adjacent strips. The projection of the amplitude signal through the two strips shows that the dead area measured at half height of the amplitude distribution is about 60 µm, Fig. 9, in agreement with the layout of the sensor.

VI. CONCLUSION

The production of UFSD 50 µm thick at FBK shows very good results. The production process used has an excellent control on the gain layer implant. The FBK first p+ implant of Gallium and the enrichment of the gain layer with Carbon was successful. These sensors have maintained the same electrical characteristics (current-voltage and Capacitance-voltage curves) and the same timing performances (jitter and time resolution) of sensors with Boron. The measurement of the dead area performed on strip sensors gave a value of ~60 µm in agreement with the production layout showing the maximum potentiality of the FBK process.

REFERENCES

[1] N. Cartiglia, *et al.*, "Design optimization of ultra-fast silicon detector", Nuclear Instrument and Method in Physics Research A, vol. 796, pp. 141-148, Oct. 2015.

[2] M. Ferrero, Il Nuovo Cimento C, "Low-gain avalanche detector activity of research and development", vol. 4, no. 70, Feb. 2017.

[3] G. Pellegrini, *et al*., "Technology development and first measurements of low gain avalanche detectors (LGAD) for high energy physics applications", Nuclear Instrument and Method in Physics Research A, vol. 795, pp. 12-16, Nov. 2014.

[4] H. F.-W. Sadrozinski, A. Seiden, N. Cartiglia, Exploring charge multiplication for fast timing with silicon sensors, 20th RD50 workshop, 30 May-1Jun. 2012.

[5] P. Fernandez, *et al*., "Simulation of new p-type strip detectors with trench to enhance the charge multiplication effect in the n-type electrodes", Nuclear Instrument and Method in Physics Research A, vol. 658, pp. 98-102, Dec. 2011.

[6] N. Cartiglia, *et al*., "Beam test results of a 16 ps timing system based on ultra-fast silicon detectors", Nuclear Instrument and Method in Physics Research A, vol. 850, pp. 83-88, Apr. 2017.

[7] G-F. Dalla Betta, et al., "Design and TCAD simulation of double-sided pixelated low gain avalanche detectors", Nuclear Instrument and Method in Physics Research A, vol. 796, pp. 154-157, Oct. 2015.

[8] G. Paternoster, *et al*., "Development and first measurements of Ultra-Fast Silicon Detector produced at FBK", Journal of Instrumentation, vol. 12, Feb. 2017.

[9] RD50 collaboration, rd50.web.cern.ch